SpezialForschungsBereich F 32

Karl–Franzens Universität Graz
Technische Universität Graz
Medizinische Universität Graz

Fast Multipole Techniques for a Mumford-Shah Model in X-Ray Tomography

E. Hoetzl, G. Of, W. Ring

SFB-Report No. 2010–034 September 2010

A–8010 GRAZ, HEINRICHSTRASSE 36, AUSTRIA

Supported by the
Austrian Science Fund (FWF)

Der Wissenschaftsfonds.

SFB sponsors:

- **Austrian Science Fund** (FWF)
- **University of Graz**
- **Graz University of Technology**
- **Medical University of Graz**
- **Government of Styria**
- **City of Graz**

Fast Multipole Techniques for a Mumford-Shah Model in X-Ray Tomography

Elena Hoetzl[a,*], Guenther Of[b], Wolfgang Ring[a]

[a] *Universitaet Graz,Institut fuer Mathematik, Heinrichstrasse 36, A-8010 Graz, Austria.*
[b] *Technische Universitaet Graz, Institut fuer Numerische Mathematik, Steyrergasse 30/III, A-8010 Graz, Austria.*

Abstract

This paper presents a numerical approach for the fast evaluation of convolution operations which occur in the problem of inversion and segmentation of X-ray tomography data via the minimization of a Mumford-Shah functional. This approach is based on ideas of the fast multipole method. The problem which we want to solve is the problem of inversion and segmentation of X-ray tomography data, using a piecewise smooth Mumford-Shah model. The numerical framework that we use is a recently developed finite difference approximation for the determination of a piecewise smooth density function as the solution of a variational problem on a variable domain. This approach achieves simultaneously the reconstruction and segmentation directly from the raw tomography data. This work focuses on the application of ideas from the fast multipole technique. The numerical analysis predicts and the numerical experiments which are presented confirm a significant speed-up of the computational time.

Keywords: inverse problems, x-ray tomography, finite difference method, level set method, shape sensitivity analysis, fast multipole method, Mumford-Shah functional
2000 MSC: 34K29, 44A12, 49M05, 65K10, 65N06, 92C50, 94A08

*Corresponding author: tel.+43 676 7110014, email: elena.hoetzl@uni-graz.at.

1. Introduction

An important task in medical imaging is to obtain information from within the human body by taking indirect measurements outside the body. In computerized tomography (CT) a measured data-set is the result of screening X-rays travelling through the body under different angles and offsets. CT is a medical imaging method which produces an image of the structures within a thin section of an object (a density function f) from a large set of one-dimensional X-ray images taken around a single axis of rotation. The mathematical relation between parameter and data is described by the Radon transform, which collects integrals of f over straight lines,

$$g_d(s,\omega) \approx Rf := \int_{\mathbb{R}} f(s\omega + t\omega^{\perp})\, dt \ ,$$

$(s,\omega) \in \mathbb{R} \times S^1$ (see [16]).

Furthermore, the planning of surgery might require the determination of the boundaries of inner organs or the separation of cancerous and healthy tissue, i.e., a segmentation of the reconstructed image is desired. Therefore as a common practice the output of the inversion method (the reconstructed density f) is used as input data for an image segmentation method to extract some specific parts within the image. In this approach, the segmentation relies only on the reconstruction and is not connected directly to the data,

$$\text{tomography data} \rightarrow \text{reconstruction of the density} \rightarrow \text{image post-processing} \rightarrow \text{segmentation} \ .$$

Such approaches with the different interpretation of the contours and with the various minimized energy functionals have been presented for the last two decades by different authors in [15, 2, 6, 10, 22, 14, 13, 4, 5, 9, 27, 21, 25].

We introduced an approach where we *do not* (as it is traditionally done) first invert the Radon transform and then segment the obtained image but we use the raw tomography data directly for both reconstruction and segmentation. Our approach, comprehensively presented in [12] and [11], achieves a simultaneous reconstruction and segmentation directly from the X-ray tomography data. The general idea was originally proposed in [23] for piecewise constant densities. In [12] we modified and improved the algorithm from [23] to allow for density functions to be not necessary piecewise constant but piecewise smooth, which gives us the possibility to treat more complicated

cases in practical applications. In our approach the optimality system is found as the necessary optimality condition for a Mumford-Shah like functional over the space of piecewise smooth densities, which may be discontinuous across the segmenting contour. Then the functional variable is eliminated by solving the optimality system for a fixed geometry. The solution is then inserted in the Mumford-Shah cost functional leading to a geometrical optimization problem for the singularity set. The resulting shape optimization problem is solved using shape sensitivity calculus and propagation of shape variables in the level-set form.

2. Mumford-Shah like functional

For a given noisy data $g_d : \mathbb{R} \times S^1 \to \mathbb{R}$, which are inaccurate measurements of ideal data $g = Rf$, the Mumford-Shah like model is designed to extract simultaneously functional and geometric information for inaccessible parameters from indirect measurements:

$$J(f, \Gamma) = \|Rf - g_d\|^2_{L^2(\mathbb{R}\times S^1)} + \alpha \int\limits_{\Omega\setminus\Gamma} |\nabla f|^2 d\mathbf{x} + \beta|\Gamma|, \tag{2.1}$$

where Γ is a geometric variable and represents the set of points on or across which the density distribution f has certain singularities. We assume that f is smooth on different parts of the body which is reasonable since in medicine, for example, the tissues of organs, muscles or bones have smooth densities. In Figure 1:

- Ω_i are sets with rectifiable boundaries
- Γ is the boundary of the individual domains
- $\Gamma = \bigcup\limits_{i=1}^{n} \partial\Omega_i = \Omega \setminus \bigcup\limits_{i=1}^{n} \Omega_i$.

3. Minimization – General Idea

The functional (2.1) contains two variables - geometric Γ and functional f. They are not completely independent since the geometry Γ is an essential part of the definition of the density function f. Therefore in the process of the minimization the functional (2.1) it is very difficult to update both those

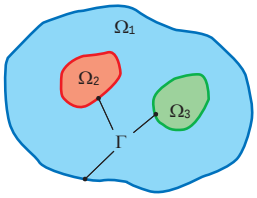

Figure 1: Domain Ω.

variables independently. As a way out we first fix Γ and solve the variational problem for the fixed Γ

$$\min_f J(f, \Gamma). \tag{3.1}$$

And then we insert the solution $f(\Gamma)$ into the Mumford-Shah like functional (2.1) and solve the shape optimization problem

$$\hat{J}(\Gamma) = \min_{\Gamma} J(f(\Gamma), \Gamma). \tag{3.2}$$

Similar approaches which use the idea of eliminating the functional variable are described in [3, 28, 9]. After solving (3.2) we find a descent direction with respect to the geometric variable Γ using shape sensitivity analysis techniques. And then, on condition that we interpret the propagation of an interface $\Gamma(t) = \{\mathbf{x} : \phi(t, \mathbf{x}) = 0\}$ as a propagation law for a corresponding time-dependent level set function $\phi(t, \mathbf{x})$, we move Γ in the chosen descent direction using a level-set methodology.

4. Solution of the optimality system for the fix geometry

The optimality system is found as the necessary optimality condition for a Mumford-Shah like functional (2.1) over the space of piecewise smooth densities. The necessary optimality conditions for the minimum f of J for fixed Γ is given as

$$\partial_f J(f(\Gamma), \Gamma)\, \phi = \langle Rf - g_d, R\phi \rangle_{L^2(\mathbb{R}\times S^1)} + \alpha \int_{\Omega\setminus\Gamma} \langle \nabla f, \nabla \phi \rangle \, d\mathbf{x} = 0$$

for all test functions $\phi \in H^1(\Omega \setminus \Gamma)$, where $\partial_f J$ denotes the derivative of J with respect to the first variable. Then the strong form of the optimality

system is given as

$$\begin{cases} R^*Rf - \alpha\Delta f = R^*g_d & \text{in} \quad \Omega \setminus \Gamma \\ \frac{\partial f}{\partial n} = 0 & \text{on} \quad \Gamma. \end{cases} \tag{4.1}$$

Since the optimality system for the fixed geometry (4.1) has the form of a coupled system of integro-differential equations on variable and irregular domains to find the solution of (4.1) becomes a non-trivial task. Also motivated by the structure of certain terms occurring in the shape derivative of the cost functional, we would like to introduce as additional unknowns, along with values of f at grid points of the finite-difference grid, also the values of f at points on the interface Γ together with the first derivatives of f at these interface points. For all those reasons in order to find the solution of the optimality system (4.1) we develop a new finite difference method based approach. We construct a consistent and numerically stable (indicating second order accuracy) scheme, where a standard five-point stencil is used on regular points of an underlying uniform grid and modifications of the standard stencil are made at points close to the boundary. These modifications concern only the construction of an approximation of the Laplace operator at boundary points and the discretization of the Neumann boundary conditions. We call points where the interface Γ crosses horizontal or vertical grid lines *intersection points*.We use a 9-points stencil approximation with a local numbering of grid points and intersection points occurring in the stencil. $k = 0$ always denotes the central grid point in the stencil. f_k denotes the value of f at a grid point with local index k. Since assembling the whole discretization matrix for the part R^*R is much too expensive in order to find an approximate solution by any iterative methods we have to apply the operators R^* and R to the previous approximation in each step of the iterative procedure. This can be achieved in reasonable time using fast rotation and interpolation. The optimality system is solved iteratively using the preconditioned Bi-CGSTAB - BiConjugate Gradient Stabilized Method. See [12] for details.

5. Shape sensitivity analysis

In our work we use techniques from shape sensitivity calculus described e.g. in [26, 7, 1, 9]. To find a descent direction for $\hat{J}$ in (3.2), we differentiate

the reduced functional $\hat{J}$ with respect to the geometry Γ to obtain:

$$d\hat{J}(\Gamma;F) = 4\sum_k \int\limits_{\mathbf{x}\in\Gamma_k} \sum_{p\in d(k)} s_p f_p(\mathbf{x}) \sum_j \int\limits_{\mathbf{y}\in\Omega_j} \frac{f_j(\mathbf{y})}{|\mathbf{x}-\mathbf{y}|}\, d\mathbf{y}\; F(\mathbf{x})\, dS(\mathbf{x}) - \quad (5.1)$$

$$-2\sum_k \int\limits_{\mathbf{x}\in\Gamma_k} \sum_{p\in d(k)} s_p f_p(\mathbf{x}) R^* g_d(\mathbf{x})\; F(\mathbf{x})\, dS(\mathbf{x}) +$$

$$+\alpha\sum_k \int\limits_{\mathbf{x}\in\Gamma_k} \sum_{p\in d(k)} |\nabla f_p(\mathbf{x})|^2\, F(\mathbf{x})\, dS(\mathbf{x}) + \beta\sum_k \int\limits_{\mathbf{x}\in\Gamma_k} \kappa(\mathbf{x})\, F(\mathbf{x})\, dS(\mathbf{x}),$$

where $s(i) = \mathrm{sign}(\phi(\mathbf{x}))$, $d(k) = \{i(k), j(k)\}$ is the set of the indices of two components Ω_i and Ω_j separated by Γ_k and $\kappa(\mathbf{x})$ is the mean curvature of Γ_k.

A direction $F : \Gamma \to \mathbb{R}$ for which the directional derivative (5.1) is negative is called a descent direction of the functional (3.2). Without loss of generality we normalize the descent direction to $\|F\| = 1$ since different scaling of the descent direction can be always compensated by the step-length's choice of the optimization algorithm. A *steepest descent direction* is a solution to the constrained optimization problem

$$\min_F d\hat{J}(\Gamma;F) \quad \text{such that} \quad \|F\| = 1. \quad (5.2)$$

It is evident from the shape sensitivity theory that the steepest descent direction $F^0_{\mathrm{sd}} : \Gamma \to \mathbb{R}$ with respect to the L^2-metric on Γ has the form

$$\begin{aligned} F^0_{\mathrm{sd}}(\mathbf{x}) = -4 \sum_{p\in d(k)} s_p f_p(\mathbf{x}) \left(\sum_j \int\limits_{\mathbf{y}\in\Omega_j} \frac{f_j(\mathbf{y})}{|\mathbf{x}-\mathbf{y}|}\, d\mathbf{y}) \right) \\ + 2 \sum_{p\in d(k)} s_p f_p(\mathbf{x}) R^* g_d(\mathbf{x}) - \alpha \sum_{p\in d(k)} |\nabla f_p(\mathbf{x})|^2 - \beta\kappa(\mathbf{x}) \end{aligned} \quad (5.3)$$

for $\mathbf{x} \in \Gamma$. (Here we omitted the normalizing factor which guarantees that $\|F^0_{\mathrm{sd}}\| = 1$.) *Note that using a second order accurate scheme as described in Section 4 is essential at this point because we need an accurate evaluation of the term* $|\nabla f_p(\mathbf{x})|$ *on* Γ_k *in* (5.3).

The level set equation of the form $\phi_t + F|\nabla\phi| = 0$ propagates simultaneously ϕ and Γ in a direction of decreasing cost functional values if F is equal to a descent direction obtained in (5.3) (this idea was proposed in [20]). The level-set equation is solved using a WENO scheme.

6. Fast Computation of the Volume Integrals by the Fast Multipole Method

The calculation of the descent direction (5.3) is computationally expensive since it involves domain integral evaluations for each single point $\mathbf{x}$ on the segmenting contour, i.e.,

$$\sum_j \int_{\mathbf{y}\in\Omega_j} \frac{f_j(\mathbf{y})}{|\mathbf{x}-\mathbf{y}|}\, d\mathbf{y}.$$

In the case of a discrete approximation of the problem based on a Cartesian grid and a quadrature rule to approximate the integral over a single square, we have to compute

$$\sum_{\ell=1}^{N} \frac{\hat{f}_\ell}{|\mathbf{x}_i-\mathbf{y}_\ell|} \tag{6.1}$$

for M evaluation points $\mathbf{x}_i$ on the contour Γ and N integration points (which will be called source points) in the domain Ω. In the case of a Cartesian $n \times n$ grid, there holds $N \in \mathcal{O}(n^2)$. For a simpler notation we use

$$\hat{f}_\ell = a(\mathbf{y}_\ell) f_j(\mathbf{y}_\ell),$$

where $a(\mathbf{y}_\ell)$ is the corresponding integration weight and j is the index such that $\mathbf{y}_\ell \in \Omega_j$. This computation requires $O(M\,N)$ arithmetical operations, i.e, in case of the Cartesian grid $\mathcal{O}(n^3)$. Therefore the evaluation of the domain integrals is the most time consuming part of the computation of the descent direction. Due to the iterative character of the overall scheme the number of such computations is very large.

For speeding up the calculations of the domain integrals, we propose to use the fast multipole method [24, 8, 17]. This method is widely used in, e.g., particle simulation and boundary element methods. In our case the computational effort is reduced from $\mathcal{O}(M\,N)$ to almost linear complexity with respect to $M+N$.

The key ideas of the fast multipole method are the separation of the variables in the kernel $|\mathbf{x}-\mathbf{y}|^{-1}$ by a series expansion and the use of an hierarchical partitioning of the points to compute the coefficients of the expansions efficiently. We will give a brief description of the main ideas of the methods; for details please see, e.g., [24, 8, 19].

First, a hierarchical cluster tree is built upon the union of the set of evaluation points $\{\mathbf{x}_i\}_{i=1}^M$ and the set of source points $\{\mathbf{y}_\ell\}_{\ell=1}^N$. A cluster ω_j^λ is a set of indices or alternatively of the corresponding points which are merged due to geometrical criterions. The domain Ω and accordingly its enclosing box contain all points and these points form a single cluster ω_1^0 of the coarsest level 0. All further clusters are created recursively by subdividing the existing clusters. The box related to a cluster ω_j^λ is subdivided into four (in 3D eight) boxes and the members of this cluster are associated to the child clusters $\omega_k^{\lambda+1}$ due to their position in one of the refined boxes. This recursive subdivision is applied up to a predefined tree depth L or until the number of points in the cluster falls below a suitable chosen limit.

Now, the computation of (6.1) is considered for pairs of clusters ω_k^λ and ω_j^λ instead of the pairs of all inclosed points to reduce the computational times. Such a pair of clusters is admissible –with respect to a low rank approximation of the corresponding part of the sum (6.1)– if

$$\operatorname{dist}\{C_k^\lambda, C_j^\lambda\} \;>\; (d+1)\max\{r_k^\lambda, r_j^\lambda\} \tag{6.2}$$

with the near-field parameter $d > 1$, the cluster centres C_j^λ and the cluster radii $r_j^\lambda = \sup_{\mathbf{x}\in\omega_j^\lambda} |\mathbf{x} - C_j^\lambda|$.

The second main idea of the fast multipole method is the separation of variables, e.g., by a Taylor series expansion. For $\mathbf{x}, \mathbf{y} \in \mathbb{R}^3$, the kernel $|\mathbf{x}-\mathbf{y}|^{-1}$ is approximated by the truncated series expansion

$$k(\mathbf{x},\mathbf{y}) = \frac{1}{|\mathbf{x}-\mathbf{y}|} \approx k_p(\mathbf{x},\mathbf{y}) = \sum_{n=0}^{p}\sum_{m=-n}^{n} \overline{S_n^m(\mathbf{y})} R_n^m(\mathbf{x}) \tag{6.3}$$

of reformulated spherical harmonics,

$$\begin{aligned} R_n^{\pm m}(\mathbf{x}) &= \frac{1}{(n+m)!}\frac{d^m}{du^m}P_n(u)|_{u=\widehat{x}_3}(\widehat{x}_1 \pm i\widehat{x}_2)^m|\mathbf{x}|^n, \\ S_n^{\pm m}(\mathbf{y}) &= (n-m)!\frac{d^m}{du^m}P_n(u)|_{u=\widehat{y}_3}(\widehat{y}_1 \pm i\widehat{y}_2)^m\frac{1}{|\mathbf{y}|^{n+1}}\,, \end{aligned}$$

where $m \geq 0$, and $\widehat{x}_i$ are the components of $\widehat{\mathbf{x}} = \mathbf{x}/|\mathbf{x}|$. Note that $x_3 = 0$ and $y_3 = 0$ hold for our problem. As we reuse an existing 3D code, we do not take advantage of this fact. In what follows, we implicitly set $x_3 = 0$ and $y_3 = 0$.

The approximation (6.3) is applied in the case that $\mathbf{x}_i$ and $\mathbf{y}_\ell$ are admissible, i.e., there exist two admissible clusters ω_j^λ and ω_k^λ such that $\mathbf{x}_i \in \omega_j^\lambda$ and $\mathbf{y}_\ell \in \omega_k^\lambda$. For a evaluation point $\mathbf{x}_i$ we define the far-field and the near-field by

$$\begin{aligned} \mathrm{FF}(i) &:= \{\ell \in \{1,\dots,N\} : \mathbf{x}_i \in \omega_k^\lambda, \mathbf{y}_\ell \in \omega_j^\lambda, \text{ and (6.2) holds}\} \\ \mathrm{NF}(i) &:= \{1,\dots,N\} \setminus \mathrm{FF}(i). \end{aligned}$$

Using the truncated series expansion (6.3), we approximate (6.1) by

$$\sum_{\ell \in \mathrm{NF}(i)} \frac{\hat{f}_\ell}{|\mathbf{x}_i - \mathbf{y}_\ell|} + \sum_{\ell \in \mathrm{FF}(i)} \hat{f}_\ell \sum_{n=0}^{p} \sum_{m=-n}^{n} \overline{S_n^m(\mathbf{y}_\ell)} R_n^m(\mathbf{x}_i).$$

After interchanging the sums we get

$$\sum_{\ell \in \mathrm{NF}(i)} \frac{\hat{f}_\ell}{|\mathbf{x}_i - \mathbf{y}_\ell|} + \sum_{\ell \in \mathrm{FF}(i)} R_n^m(\mathbf{x}_i) \widetilde{L}_n^m(\mathrm{FF}(\ell)), \tag{6.4}$$

where

$$\widetilde{L}_n^m(\mathrm{FF}(\ell)) = \sum_{\ell \in FF(i)} \hat{f}_\ell \overline{S_n^m(\mathbf{y}_\ell)}. \tag{6.5}$$

If the coefficients $\widetilde{L}_n^m$ are known, an approximation of the domain integrals can be computed by (6.4) with $\mathcal{O}(M\,p^2)$ operations. Note that the number of source points in the near-field of an evaluation point can be bounded by a constant or by $\mathcal{O}(p^2)$ using a suitable cluster tree.

The coefficients $\widetilde{L}_n^m$ of (6.5) depend on the far-field $\mathrm{FF}(\ell)$. In general, these far-fields do not coincide for different evaluation points. The fast multipole method provides a sophisticated algorithm based on the cluster tree to compute these coefficients with almost linear complexity. The idea is to compute these coefficients for pairs of admissible clusters instead of for each pair of a source point and an evaluation point. For pairs of clusters on a coarser level of the tree, the reduction of the computational effort is even larger. The algorithm combines the coefficients of pairs of admissible clusters in such a way that finally the coefficients $\widetilde{L}_n^m$ for all different far-fields $\mathrm{FF}(\ell)$ are computed. The description of the complete algorithm is beyond the focus of this paper; please see, e.g., [8, 19] for details.

In the case of the considered volume integrals, the overall computational effort is of $\mathcal{O}((M+N)p^2)$, where the expansion degree p controls the error

of the approximation of the volume potentials defined by the fast multipole method, see e.g. [18]. A choice of $p \sim \log N$ is sufficient to preserve the order of convergence of the full method.

7. Numerical Results

The necessary tomography test data $g_d(s, \omega)$ was created synthetically using a piecewise smooth density distribution f as input. The image for the density has a size of 201×201 pixels and contains three regions (see Figure 2 left). The measurements were simulated over the full circle for 319 angles and 320 offsets.

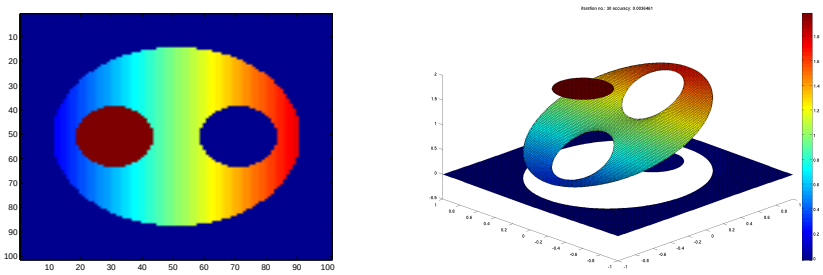

Figure 2: Density distribution f (left) and reconstructed (exact) density distribution (right).

The reconstruction of the density distribution from (numerically) exact data using the technique proposed in this work are shown in Figure 2 (right). One can see no difference the reconstructed density with the original one. In Figure 3 (left-hand side) the initial guess (red contour), the propagating contour (blue contour) and the exact geometry (black contour) are shown. The algorithm is quite stable with respect to the correct detection of all objects in the image and does not produce persistent false contours. We needed 392 iterations to arrive at the final result. The corresponding reconstructed density is shown on the right-hand side.

In Figure 4 (right-hand side) reconstructed contours are presented where the exact data are contaminated with 20% of Gaussian noise (100 iterations). One can hardly notice the difference with the noise-free reconstruction for the contours (left-hand side) (51 iterations). But the corresponding density reconstruction in Figure 5 is slightly worse which is reasonable taking into account 20% of noise.

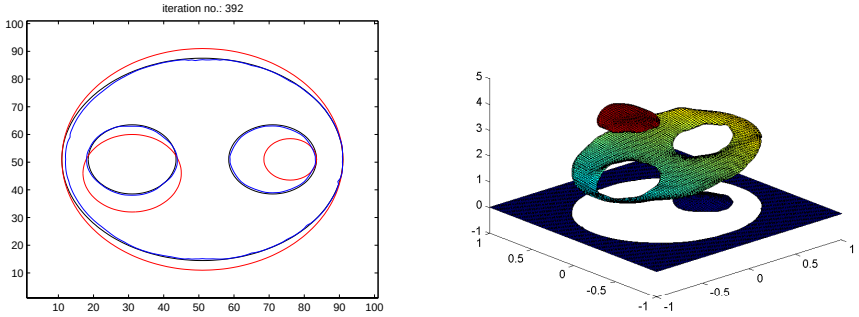

Figure 3: Reconstruction of Γ without precondition $\alpha = 0.08$, $\beta = 0.3$ (left) (red contour is the initial guess, blue is the propagating contour, black contour is the exact geometry) and corresponding reconstructed density (right).

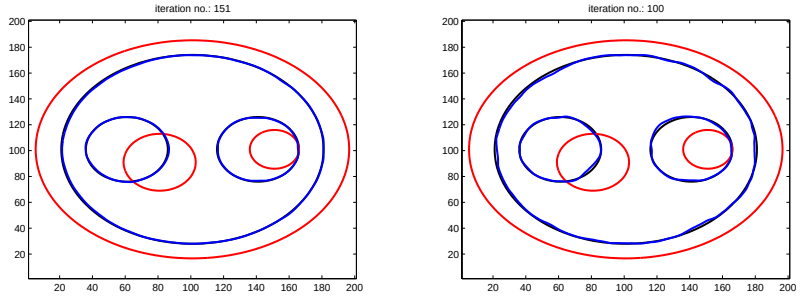

Figure 4: Reconstruction of Γ $\alpha = 0.1$, $\beta = 0.1$ from the noise-free data (left) and from the noisy data (20%) (right) $\alpha = 0.3$, $\beta = 0.3$.

Our experiments showed that the algorithm is quiet flexible with respect to topological changes especially if the initial topology is sufficiently complex. It is also reliable with respect to the contrast between the different partitions of the underlying domain. Our approach achieves very good quality of the reconstruction and segmentation directly from X-ray data.

Of course, as a natural expectation in practical applications, the computational time and memory requirement play an important role. Our experiments show a significant speed-up of the computations of the volume integrals using the fast miltipole technique. In Table 6 the computational times of the straightforward implementation are compared to those of the fast multipole method for a single evaluation of the volume integral in (5.3). Data size is the number of nodes of the Cartesian grid. We already observe

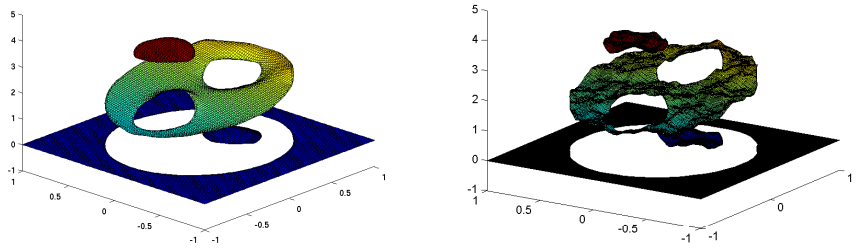

Figure 5: Reconstructed density $\alpha = 0.1$, $\beta = 0.1$ from the noise-free data (left) and from the noisy data (20%) (right).

a speed-up for the smallest example. For larger examples the speed-up gets significant due to the better asymptotic behaviour of fast multipole method.

data size	without FMM(sec)	with FMM(sec)	speed-up
101×101	0.21	0.06	≈ 3.5
201×201	1.5	0.17	≈ 8.82
401×401	11.89	0.46	≈ 25.85
667×667	54.96	1.18	≈ 46.58
1001×1001	185.46	3.11	≈ 59.63

Figure 6: Comparison of the time spent for the Fast Multipole Method (FMM) and straight forward calculations.

Interestingly the evolution of the cost function values over the iteration steps of the algorithm is much better for the fast multipole implementation than for the standard implementation. In Figure 7 a comparison of the cost function values is shown. The cost functional values decrease much faster for the fast multipole implementation. The final values of the cost functional where the quality of the reconstruction is not improved any more are approximately of the same magnitude. We attribute the faster convergence of the fast multipole implementation to a regularizing effect which comes from the dimensional reduction that is inherent in the fast multipole approximation.

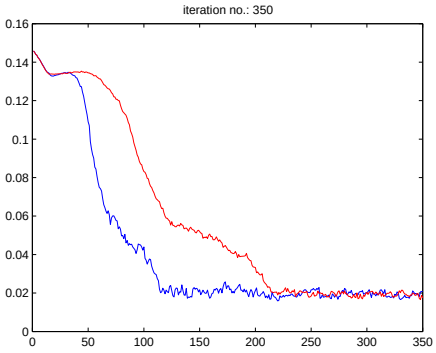

Figure 7: Cost function values over the iteration for the fast multipole implementation (blue) and the standard implementation (red).

8. Conclusion

In this work we introduced a fast multipole method based approach for the fast evaluation of convolution operations and other integral representations of expressions which (inevitably) occur in the shape gradient of a Mumford-Shah model for X-ray tomography. Using the ideas of the fast multipole method in our algorithm is an another new way of looking at the problem of domain integral evaluation in context of the tomography problems. An implementation of the fast multipole technique in our algorithm seems to be extremely promising in reducing the computational time and memory requirement. Moreover this approach can be used for - more importantly in medical applications - SPECT reconstruction. Also for 3-D reconstruction an acceleration of the computational time is essential for the success of the reconstruction process and comply with the goal of this work.

References

[1] Gilles Aubert, Michel Barlaud, Olivier Faugeras, and Stéphanie Jehan-Besson. Image segmentation using active contours: calculus of variations or shape gradients? *SIAM J. Appl. Math.*, 63(6):2128–2154 (electronic), 2003.

[2] Vicent Caselles, Francine Catté, Tomeu Coll, and Françoise Dibos. A geometric model for active contours in image processing. *Numer. Math.*, 66(1):1–31, 1993.

[3] T. F. Chan and L. A. Vese. A level set algorithm for minimizing the Mumford-Shah functional in image processing. UCLA CAM Report 00-13, University of California , Los Angeles, 2000.

[4] T. F. Chan and L. A. Vese. Active contours without Edges. *IEEE Trans. Image Processing*, 10(2):266–277, 2001.

[5] T. F. Chan and L. A. Vese. A multiphase level set framework for image segmentation using the Mumford and Shah model. *Int. J. Comp. Vision*, 50(3):271–293, 2002.

[6] L. D. Cohen and R. Kimmel. Global minimum for active contour models: a minimum path approach. *International Journal of Computer Vision*, 24(1):57–78, 1997.

[7] M. C. Delfour and J.-P. Zolésio. *Shapes and geometries*. Society for Industrial and Applied Mathematics (SIAM), Philadelphia, PA, 2001. Analysis, differential calculus, and optimization.

[8] L. Greengard and V. Rokhlin. A fast algorithm for particle simulations. *J. Comput. Phys.*, 73:325–348, 1987.

[9] M. Hintermüller and W. Ring. An inexact Newton-CG-type active contour approach for the minimization of the Mumford-Shah functional. *J. Math. Imag. Vis.*, 20(1–2):19–42, 2004.

[10] Michael Hintermüller and Wolfgang Ring. A second order shape optimization approach for image segmentation. *SIAM J. Appl. Math.*, 64(2):442–467 (electronic), 2003/04.

[11] E. Hoetzl and W. Ring. An active contour approach for a Mumford-Shah model in X-ray tomography. *Advances in Computing Sciences, Springer Lecture Notes in Computer Science*, LNCS 5876:1021 ff., 2009.

[12] E. Hoetzl and W. Ring. Numerical treatment of the mumford-shah model for the inversion and segmentation of x-ray tomography data. *Inverse Problems in Science and Engineering*, 18(7):907–933, 2010.

[13] S. Jehan-Besson, M. Barlaud, and G. Aubert. DREAM^{2}S: Deformable regions driven by an Eulerian accurate minimization method for image and video segmentation. November 2001.

[14] S. Jehan-Besson, M. Barlaud, and G. Aubert. Video object segmentation using Eulerian region-based active contours. In *International Conference on Computer Vision, Vancouver*, July 2001.

[15] M. Kass, A. Witkin, and D. Terzopoulos. Snakes: Active contour models. *Int. J. of Computer Vision*, 1:321–331, 1987.

[16] F. Natterer. *The Mathematics of Computerized Tomography*, volume 32 of *Classics in Applied Mathematics*. Society for Industrial and Applied Mathematics (SIAM), Philadelphia, PA, 2001. Reprint of the 1986 original.

[17] N. Nishimura. Fast multipole accelerated boundary integral equation methods. *Applied Mechanics Reviews*, 55(4):299–324, 2002.

[18] G. Of, O. Steinbach, and P. Urthaler. Fast evaluation of volume potentials in boundary element methods. *SIAM J. Sci. Comput.*, 32(2):585–602, 2010.

[19] G. Of, O. Steinbach, and W. L. Wendland. The fast multipole method for the symmetric boundary integral formulation. *IMA J. Numer. Anal.*, 26(2):272–296, 2006.

[20] Stanley Osher and James A. Sethian. Fronts propagating with curvature-dependent speed: algorithms based on Hamilton-Jacobi formulations. *J. Comput. Phys.*, 79(1):12–49, 1988.

[21] Stanley J. Osher and Ronald P. Fedkiw. *Level Set Methods and Dynamic Implicit Surfaces*. Springer Verlag, New York, 2002.

[22] N. Paragios and R. Deriche. Geodesic active regions: a new paradigm to deal with frame partition problems in computer vision. *International Journal of Visual Communication and Image Representation*, 2001. To appear in 2001.

[23] R. Ramlau and W. Ring. A Mumford-Shah level-set approach for the inversion and segmentation of X-ray tomography data. *J. of Comput. Phys.*, 221, issue 2:539–557, 2007.

[24] V. Rokhlin. Rapid solution of integral equations of classical potential theory. *J. Comput. Phys.*, 60:187–207, 1985.

[25] J. A. Sethian. *Level set methods and fast marching methods*. Cambridge University Press, Cambridge, second edition, 1999. Evolving interfaces in computational geometry, fluid mechanics, computer vision, and materials science.

[26] J. Sokołowski and J-P. Zolésio. *Introduction to shape optimization*. Springer-Verlag, Berlin, 1992. Shape sensitivity analysis.

[27] Demetri Terzopoulos. Deformable models: classic, topology-adaptive and generalized formulations. In *Geometric level set methods in imaging, vision, and graphics*, pages 21–40. Springer, New York, 2003.

[28] A. Tsai, A. Yezzi, and A. S. Willsky. Curve evolution implementation of the Mumford-Shah functional for image segementation, denoising, interpolation, and magnification. *IEEE Trans. Image Process.*, 10(8):1169–1186, 2001.